HHS Public Access

Author manuscript

Biomaterials. Author manuscript; available in PMC 2016 June 01.

Published in final edited form as:

Biomaterials. 2015 June ; 53: 731–743. doi:10.1016/j.biomaterials.2015.02.082.

Nanoparticle formulation of ormeloxifene for pancreatic cancer

Sheema Khan[a,†], **Neeraj Chauhan**[a,†], **Murali M. Yallapu**[a,†], **Mara C. Ebeling**[b], **Swathi Balakrishna**[a], **Robert T. Ellis**[c], **Paul A. Thompson**[d], **Pavan Balabathula**[e], **Stephen W. Behrman**[f], **Nadeem Zafar**[g], **Man Mohan Singh**[h], **Fathi T. Halaweish**[i], **Meena Jaggi**[a], and **Subhash C. Chauhan**[a,*]

[a]Department of Pharmaceutical Sciences and Center for Cancer Research, University of Tennessee Health Science Center, Memphis, Tennessee, USA

[b]Cancer Biology and Sanford Children's Health Research Center, Sanford Research/USD, Sioux Falls, South Dakota, USA

[c]College of Medicine, University of Tennessee Health Science Center, Memphis, Tennessee, USA

[d]Methodology and Data Analysis Center, Sanford Research, Sioux Falls, South Dakota, USA

[e]Department of Pharmaceutical Sciences and Plough Center for Sterile Drug Delivery, University of Tennessee Health Science Center, Memphis, Tennessee, USA

[f]Department of Surgery, University of Tennessee Health Science Center, Memphis, Tennessee, USA

[g]Department of Pathology, University of Tennessee at Memphis, Memphis, Tennessee, USA

[h]Saraswati Dental College, Lucknow, Uttar Pradesh, India

[i]Department of Chemistry & Biochemistry, South Dakota State University, Brookings, SD 57007, USA

Abstract

Pancreatic cancer is the fourth most prevalent cancer with about an 85% mortality rate; thus, an utmost need exists to discover new therapeutic modalities that would enhance therapy outcomes of this disease with minimal or no side effects. Ormeloxifene (ORM), a synthetic molecule, has exhibited potent anti-cancer effects through inhibition of important oncogenic and proliferation

[*]**Corresponding Author:** Subhash C. Chauhan, Ph.D., Professor, Department of Pharmaceutical Sciences, University of Tennessee Health Science Center, 19 South Manassas, Cancer Research Building, Memphis, TN, 38163. Phone: (901) 448-2175. Fax: (901)-448-1051. schauha1@uthsc.edu.

[†]**Equal Contributors:** Sheema Khan, Neeraj Chauhan, Murali M. Yallapu

Conflicts of Interest

The authors do not have any conflict of interest in this work. NC, MMY, MJ, and SCC have jointly filed a United States Provisional Patent Application, Serial No. 62/030,971, for "NANOFORMULATIONS FOR CANCER" based on the studies reported in this manuscript.

signaling pathways. However, the anti-cancer efficacy of ORM can be further improved by developing its nanoformulation, which will also offer tumor specific targeted delivery. Therefore, we have developed a novel ORM encapsulated poly(lactic-*co*-glycolic acid) nanoparticle (NP) formulation (PLGA-ORM NP). This formulation was characterized for particle size, chemical composition, and drug loading efficiency, using various physico-chemical methods (TEM, FT-IR, DSC, TGA, and HPLC). Because of its facile composition, this novel formulation is compatible with antibody/aptamer conjugation to achieve tumor specific targeting. The particle size analysis of this PLGA-ORM formulation (~ 100 nm) indicates that this formulation can preferentially reach and accumulate in tumors by the Enhanced Permeability and Retention (EPR) effect. Cellular uptake and internalization studies demonstrate that PLGA-ORM NPs escape lysosomal degradation, providing efficient endosomal release to cytosol. PLGA-ORM NPs showed remarkable anti-cancer potential in various pancreatic cancer cells (HPAF-II, BxPC-3, Panc-1, MiaPaca) and a BxPC-3 xenograft mice model resulting in increased animal survival. PLGA-ORM NPs suppressed pancreatic tumor growth *via* suppression of Akt phosphorylation and expression of MUC1, HER2, PCNA, CK19 and CD31. This study suggests that the PLGA-ORM formulation is highly efficient for the inhibition of pancreatic tumor growth and thus can be valuable for the treatment of pancreatic cancer in the future.

1. Introduction

Pancreatic cancer is one of the most deadly malignancies in the United States [1, 2]. Despite advances in the field of surgery, chemotherapy, and radiation therapy, the prognosis of pancreatic cancer remains extremely poor with a 1- to 5-year overall survival rate of about 25% and 6%, respectively, which is the lowest among common malignancies [3]. None of the current chemotherapy regimens provide more than one-year survival benefit. Gemcitabine is the most commonly used chemotherapy for pancreatic cancer, which improves overall survival rate by about 6.7 months. A recent FDA approved combination treatment regimen of Abraxane® (a human serum-bound paclitaxel nanoparticle formulation) with gemcitabine has only increased overall survival to 8.5 months. Therefore, it is imperative to develop new chemotherapeutic approaches to further improve the clinical outcome of pancreatic cancer patients. Many new drug(s) and drug combination based therapeutic regimens have resulted in poor patient tolerance, drug's low half-life, low cellular uptake, and high systemic toxicity [4–7]. Such therapeutic options largely fail in Phase II or Phase III trials and thus cause huge financial burdens. Thus, repurposing of drugs that are already approved for human use for other indications seems to be a promising new treatment option for cancer [8–10]. The advantages of such strategy are fewer restrictions by FDA for clinical trials and the possibility of rapid translation to the clinic. A recent example of drug repurposing is metformin (a drug for diabetes treatment), which has shown potent cancer chemopreventive and chemotherapeutic activities [11–13]. Ormeloxifene (ORM), a non-steroidal molecule which is widely used as an oral contraceptive in humans [14, 15], can be repurposed for cancer treatment. This is a potent agent that has been widely shown to act upon several important molecular targets in cancer [16]. ORM has shown greater protective effects on *Salmonella* strains TA97a, TA98, TA100 and TA102 than Tamoxifen [17]. Interestingly, ormeloxifene induces significant tumor growth inhibition in rat model [17]. More importantly, a Phase II clinical study in 70 female patients, achieved ~38.7%

overall response rate with 6 months of ormeloxifene treatment [18]. Recent studies from our lab and others suggest an anti-tumorigenic effect of ORM in various cancers, such as ovarian, breast, head and neck, and chronic myeloid leukemia [18–24]. Its inhibitory activity of highly tumorigenic and metastatic pancreatic cancer cells provides strong rationale to implement this molecule for anti-cancer applications. Another reason for choosing this molecule for cancer therapeutics is because it exhibits excellent therapeutic index with no systemic toxicity at chronic administration [25]. All these studies indicate that ormeloxifene is an excellent drug candidate for cancer treatment.

Pancreatic ductal adenocarcinoma exhibits several pathological features that lead to disorganized, leaky and nonfunctional vasculature [26–28], dense stroma [29], and deregulated cellular transport proteins [30]. This leads to ineffective drug delivery and drug resistance by creating high interstitial fluid pressure [31], preventing the movement of chemotherapy from the vasculature to the extracellular compartment. This complexity suggests that an efficient delivery of ormeloxifene is highly desirable to effectively eradicate pancreatic cancer cells. Delivery of drugs using nanocarrier(s) can easily pass the pores in leaky endothelial cells ranging as low as 100 to 780 nm [32, 33] and result in clusters around the neoplastic cells and prolonged drug release. Poly(lactide-*co*-glycolide) (PLGA) is an FDA-approved biodegradable and biocompatible polymer employed for controlled drug delivery applications including anti-cancer drug delivery [34, 35]. We, along with other labs, have shown that using PLGA nanoparticles to deliver chemotherapeutic drugs results in significant improvement in inhibition of tumor burden in a wide variety of cancer models [36–38]. Therefore, in the present study, an ORM-loaded PLGA nanoparticle (PLGA-ORM NP) formulation was prepared by co-precipitation technique and characterized by TEM, FTIR, DSC, TGA, and HPLC for evaluating particle size, drug loading, and formulation identification. The internalization and fate of PLGA-ORM NPs in pancreatic cancer cells was observed by confocal microscopy. The anti-proliferative effect of PLGA-ORM NPs was analyzed and compared with free ORM by MTS and clonogenic potential assays. We observed the modulation of key oncogenic targets in pancreatic cancer cells by PLGA-ORM NPs. Additionally, the PLGA-ORM NPs effectively inhibited pancreatic tumorigenesis in a xenograft mouse model.

2. Materials and Methods

2.1. Chemicals and antibodies

PLGA copolymer (50:50 lactide–glycolide ratio; inherent viscosity 1.32 dL/g at 30°C) was purchased from Birmingham Polymers (Pelham, AL). Propidium iodide (PI), MTS [3-(4,5-dimethylthiazol-2-yl)-5-(3-carboxymethoxyphenyl)-2-(4-sulfophenyl)-2H-tetrazolium, inner salt)], Phenylmethanesulfonyl fluoride (PMSF), fetal bovine serum, eukaryotic protease inhibitor cocktail, and pyruvic acid were purchased from Sigma–Aldrich Co. (St. Louis, MO) or Fisher Scientific (Pittsburgh, PA). All chemicals and reagents were used without further purification. Mouse anti-human monoclonal antibodies to MUC1 and rabbit anti-human antibodies to HER2, Cytokeratin 19, p27, PTEN, Cyclin D1, p-Akt, Survivin, Bax, and Caspase-3 were purchased from Cell Signaling Laboratory. The rabbit anti-human antibody to CD31 was purchased from Abcam (Cambridge, MA). The anti-mouse IgG HRP

and rabbit IgG HRP-linked secondary antibodies were procured from Promega (Madison, WI). The hematoxylin stain was purchased from Fisher Scientific and the Annexin V/FITC apoptosis kit from Bio-Rad (Hercules, CA).

2.2 Cell culture, growth conditions, and treatment

Cell lines were grown in specific media (HyClone Laboratories, Inc., Grand Island, NY) that is routinely used to culture them in our laboratory. HPAF-II cells were cultured in DMEM/F12, BxPC-3 and AsPC-1 cells in RPMI 1640 and Panc-1 cells in DMEM medium. Additionally, the medium was supplemented with 10% FCS, 100 U penicillin/100 μg streptomycin per mL medium. Cells were grown in a CO_2 incubator (Thermocon Electron Corporation, Houston, TX) at 37°C with 98% humidity and 5% CO_2 gas environment. Cells grown in monolayer cultures were detached with trypsin (0.1%, w/v)/EDTA (1 mM) solution. Cells were dispersed gently by pipetting in complete growth medium, and centrifuged at 200 g for 5 min. Cells were dispersed in complete medium in culture flasks and incubated in a CO_2 incubator. Cells grown in semi-confluent stage (~70% confluent) were treated with PLGA NPs, PLGA-ORM NPs or free ORM while the untreated control cultures received only the vehicle (ethanol <0.2%, v/v).

2.3. Synthesis of PLGA-ORM NPs

PLGA-ORM NPs were prepared by following a nano-precipitation technique [36, 37] with a modified protocol. The stable PLGA-ORM NP suspension was obtained using polymer stabilizers, poly(vinyl alcohol) (PVA) and poly(L-lysine) (PLL). Briefly, to 20 mL aqueous 1% PVA solution, 90 mg of PLGA and 20 mg ORM were dissolved in 8–10 mL acetone that was added drop-wise using a 1 mL pipette over 10 min under constant stirring on a magnetic stir plate at 500 rpm. This process leads to a milky-white suspension. This suspension was left overnight at room temperature in the chemical fume hood under stirring condition, allowing for complete evaporation of the acetone. Then, to this suspension, 10 mg PLL in 5 mL water was added and stirred at 500 rpm for 6 h. The resulted PLGA-ORM NPs in suspension were purified and recovered by ultracentrifugation at 20,000 rpm for 2 h at 4°C, three times, using a Rotor 30.50 on an Avanti J-30I Centrifuge (Beckman Coulter, Fullerton, CA), followed by re-suspension in ultra-purified water and sonication on ice for 1 min (using a probe sonicator). Then the supernatant containing PLGA-ORM NPs was transferred to a sterile cryo-vial, frozen at −80°C for 2 h, and immediately lyophilized for 2–3 days using the Labconco Freeze Dry System (−48°C, 133×10^{-3} mBar; Labconco, Kansas City, MO). The lyophilized vials were stored in a 4°C cold room for further *in vitro* and *in vivo* use. This formulation was named PLGA-ORM20. Similarly, PLGA-ORM formulations with 5, 10, 15, and 25 mg ORM were prepared and termed as PLGA-ORM5, PLGA-ORM10, PLGA-ORM15, and PLGA-ORM25, respectively. Additionally, parent PLGA NPs were also prepared without ORM that can serve as a control for all *in vitro* and *in vivo* experiments. The PLGA-ORM 20 formulation was used for all *in vitro* and *in vivo* experiments. In the results and discussion sections the PLGA-ORM 20 formulation was designated as PLGA-ORM NPs.

2.4. PLGA-ORM NPs characterization

2.4.1. Particle size—PLGA-ORM NPs were characterized for the surface morphology and size of particles using a JEOL-1210 transmission electron microscope (TEM) (JEOL Ltd., Tokyo, Japan) operating at 60 kV. For this, 50 μL suspension of 1 mg/mL PLGA-ORM NPs was carefully dispersed on 200 mesh formvar-coated copper TEM-grid (grid size: 97 μm) (Ted Pella, Inc., Redding, CA), followed by staining with 2% w/v of uranyl acetate solution. The excess solution on the grid was removed by air drying. Then, particles on the TEM-grid were imaged under TEM.

2.4.2. Drug loading—To determine ORM loading, freshly prepared PLGA-ORM NPs were centrifuged three times at 20,000 rpm for 2 h at 4°C using an Avanti J-30I Centrifuge, followed by re-suspension in ultra-purified water and sonication on ice for 1 min. The supernatant was removed, the pellet was re-suspended, lyophilized, and ORM was extracted from pellet for 2 days with 1 mL of acetonitrile. The concentration of ORM in the extract was analyzed using an UltiMate high-performance liquid chromatography (HPLC) (Dionex Corporation) equipped with an UltiMate 3000 injector, RS variable wavelength detector, and an Acclaim polar advantage column of 3 μm 120 Å (4.6 × 150 mm). The mobile-phase consisted of a mixture of 1% citric acid:acetonitrile (40:60, v/v). 50 μL of the extracted samples was injected using an auto injector (Model 508, Beckman Instruments) and peaks were analyzed using a UV detector at 279 nm [39]. A linear calibration curve in the range of 1 to 10 μg/mL was obtained at the same working condition to calculate ORM loading.

2.4.3. Fourier Transform infra-red—FT-IR spectra of PLGA-ORM NPs were obtained using a Fourier Transform infra-red (FT-IR) microscope (Smiths Detection, Danbury, CT). The spectra data, 4,000–750 cm^{-1}, was acquired at a scanning speed of cm^{-1} for 32 scans by placing lyophilized PLGA-ORM NPs powder on the attenuated total reflection objective. The final data is reported as an average data of 32 scans.

2.4.4. Thermal analysis—Thermal analysis of PLGA-ORM NPs was carried out using a differential scanning calorimetry (DSC) and thermo-gravimetric analyzer (TGA) to investigate the physical status and thermal profile. Both DSC and TGA profiles were accomplished on a Q50 TGA (TA Instruments, New Castle, DE) under dry nitrogen atmosphere (a flow rate of 10 mL/min) from 25°C to 700°C at the heating rate of 10°C/min.

2.5. Cellular uptake

PLGA-ORM20 NP formulation was evaluated for cellular uptake and internalization. In brief, 500 μg 6-coumarin in acetone was mixed with 90 mg of PLGA and 20 mg ORM in 8 mL acetone, and added drop-wise to 20 mL aqueous 1% PVA solution to obtain final 6-coumarin labeled PLGA-ORM20 NPs. Dye (6-coumarin) labeling in PLGA-ORM20 NPs was confirmed using fluorescence spectra and fluorescence microscope, before continuing for internalization/uptake studies in cells. This formulation enabled us to detect green fluorescence in cells to track/identify internalization/uptake of NPs in cells. The cellular fate of PLGA-ORM20 NPs in HPAF-II cells was observed by using confocal microscopy. For immunofluorescence experiment, HPAF-II cells (1×10^5/well) were grown on 4-well chamber glass slides and allowed to attach overnight prior to the addition of 6-coumarin

loaded PLGA-ORM NPs or respective controls. Then, cells were washed twice with PBS, fixed in 2% paraformaldehyde (50 μg) for 10 min and permeabilized with 0.1%TritonX-100 in PBS for 10 min. After a blocking step with 2% goat serum in PBS for 1 h, the cells were incubated at 4°C for 1 h with 30 nM Mito Tracker Red or 50 nM Transferrin from Human Serum, Texas Red® Conjugate or 75 nM LysoTrackerR Red DND-99 (Life Technologies) to stain as a marker for mitochondria, endosome, and lysosome, respectively. Nuclei were stained with DAPI (4',6-diamidino-2-phenylindole, Life Technologies). Images were acquired at 1024 pixel resolution and 600× magnification using a laser confocal microscope (Nikon Corporation).

2.6. Cell proliferation assay

MTS growth inhibition method [40] was performed to assess cytotoxicity of PLGA-ORM NPs and ORM. Pancreatic cancer cells (5.0×10^3/200 μL media/96-well culture plates) were treated with different concentrations of PLGA-ORM NPs and ORM to determine their effect on cell proliferation. Appropriate equivalent amounts of ethanol or PLGA in PBS were used as controls. Each treatment condition was replicated six times. After incubation for 48 h, MTS dye was added to the cells and incubated for 2 h at 37°C. Absorbance was measured at 490 nm. Cell growth as percent viability was calculated by comparing the absorbance of treated versus untreated cells. The percentage of cell growth was calculated as the percentage of the absorption of treated cells to the absorption of non-treated cells.

2.7. Clonogenic assay

Clonogenic assay or colony formation assay is an *in vitro* cell survival assay based on the ability of a single cell to grow into a colony. Various pancreatic cancer cells treated with indicated concentrations of PLGA-ORM NPs and ORM (5×10^3/6 well culture plate) were seeded in appropriate dilutions to form colonies for two weeks. Visible colonies (~50 cells) were manually counted as discussed earlier [41]. The results are presented as percentage of colonies as compared to the vehicle control (ethanol/PLGA NPs).

2.8. Western blotting

Whole-cell lysates from cells were prepared as described earlier [42]. The protein from tumor tissues was isolated by first homogenizing 40–70 mg tissue in Tissue Extraction reagent-1 (Life Technologies) followed by centrifugation at 12000 g for 10 min. The supernatant was collected and stored for protein estimation as determined by Bradford assay, resolved on SDS-PAGE, and immunoblotted as described earlier [39].

2.9. Anti-tumor efficacy

Six-week-old female athymic nude (nu/nu) mice were purchased from Charles River Laboratories International, Inc. (Wilmington, MA), and maintained in a pathogen-free environment. To establish BXPC-3 tumor xenografts, BxPC-3 cells (5×10^6) were dispersed in 100 μL PBS/Matrigel matrix and subcutaneously inoculated into the mice at the right flank. Additionally, 3×10^6 BxPC-3 cells were injected intraperitoneally to achieve tumor metastasis. On day 15, the mice were treated with vehicle (PLGA) or PLGA-ORM NPs (200 μg), *via* intraperitoneal (ip) injections, thrice a week, for six subsequent weeks. Mice were

weighed twice a week to monitor their health and tumor growth. Tumor volume (V) was estimated from the length (l), width (w), and height (h) of the tumor using the formula V = ¼ 0.52(l × w × h), as described previously [43]. Mice were euthanized 45 days after the first drug injection, and tumor burden (wet weight) and metastases were recorded. The organs, including pancreas, were harvested and checked for metastases. Primary analyses involved planned comparisons (separately for each time point) between control PLGA vs. PLGA-ORM 20 NPs. Animal care was performed in accordance with institutional guidelines and the Institutional Animal Care and Use Committee (IACUC) approved the protocols used.

2.10. Immunohistochemistry

To further characterize the cellular expression of various proteins in the xenograft tumor tissue slides from PLGA and PLGA-ORM 20 treated mice, we used heat-induced antigen retrieval immunohistochemistry technique with the Biocare kit (Biocare Medical, Concord, CA) [44]. Briefly, slides containing the tumor tissues were deparaffinized, rehydrated, treated with 0.3% hydrogen peroxide or peroxidazed solution (Biocare Medical) and processed for antigen retrieval using heat-induced technique. After blocking nonspecific binding with background sniper (Biocare Medical), the tissues were incubated with specific antibodies at recommended concentrations. For the final detection of protein using chromogenic dyes 3,3′-diaminobenzidine (DAB), the samples were processed using a MACH 4 Universal HRP Polymer detection kit (Biocare Medical) according to manufacturer's instructions and developed using DAB (DAB substrate kit, Vector Laboratories, Burlingame, CA). The slides were visualized through a bright field microscope.

2.11. Statistical analysis

The data are presented as means ± S.E.M. of several independent experiments. The *p*-values <0.05 were considered statistically significant. All statistical analyses were performed using the Statistical Package for the Social Sciences, version 11.5 (SPSS Inc., Chicago, IL).

3. Results

The main aim of this study was to improve the anti-cancer activity of ORM using a nanoparticle formulation (Figure 1A), and to examine its efficacy in human pancreatic cancer cell line and xenograft mouse models. The motive to make an ORM nanoformulation is that NPs are known to preferentially reach and accumulate in tumor tissue(s) due to leaky vasculature by the Enhanced Permeation and Retention (EPR) effect [45, 46]. Abraxane® is an example of a NP which harnesses the EPR effect and has been widely used in the clinic for the treatment of various types of cancers, including pancreatic cancer. Abraxane's effectiveness confirms that nanodrug formulation(s) may have superior outcome over traditional chemotherapy in clinical oncology. Therefore, we have generated a PLGA-based ORM nanoparticle formulation, PLGA-ORM NPs. The selection of the PLGA NP-based formulation to deliver ORM is due to the fact that the PLGA co-polymer has shown promising results in *in vitro*, *in vivo* animal, pre-clinical, and human studies (for example, BIND-014, a docetaxel PLGA NP formulation). Based on these facts, we have engineered an optimized PLGA-ORM NP formulation, composed of a PLGA core that is subsequently

coated with poly(vinyl alcohol) (PVA) and poly(l-lysine) (PLL) for efficient delivery and targeting of ORM to cancer cells. This formulation (Figure 1A), has several unique properties: *(a)* the PLGA core is capable of loading and releasing ORM in a sustained manner, and more importantly, it was approved by US Food and Drug Administration, *(b)* PVA, a widely used stabilizer for most of the polymer NP formulation(s), supports stability of the formulation over 6 month(s) and avoids non-specific adsorption of human serum proteins in *in vivo* condition, *(c)* PLL promotes cellular internalization and is less toxic compared to other polycationic polymers, and *(d)* amine functional groups on NPs (PLL) are useful for antibody conjugation through a PEG-linker, notably the N-hydroxysuccinimide (NHS) group, for targeting tumor/cancer cells. Therefore, we used this formulation for ORM delivery to human pancreatic cancer cells and tumors in a BxPC-3 xenograft mouse model.

3.1. Characterization of PLGA-ORM NPs

PLGA and PLGA-ORM NP formulations (PLGA-ORM5, PLGA-ORM10, PLGA-ORM15, PLGA-ORM20, and PLGA-ORM25) were successfully prepared by increasing amounts of ORM in the composition (0 to 25 mg). Drug loading was assessed by HPLC method that indicated all the nanoformulations resulted in ORM encapsulation (> 80–90% encapsulation efficiency). All formulations exhibit homogeneous spherical shapes and smooth surfaces without cracks (Fig 1B). The mean particle size of PLGA or PLGA-ORM NPs was found to be 30.8 ± 1.5 nm (PLGA NPs), 68.4 ± 1.5 nm (PLGA-ORM5), 70.8 ± 4.5 nm (PLGA-ORM10), 87.3 ± 1.5 nm (PLGA-ORM15), 101.4 ± 1.5 nm (PLGA-ORM20), and 175.2 ± 1.5 nm (PLGA-ORM25) (Fig. 1C). The size of PLGA-ORM NP formulations was mostly between 50 nm to 250 nm and was narrowly distributed in each formulation. It was noticed that the formulation particle size increased when drug loading used for the particle preparation increased. However, all these formulations were small enough in size and suitable for tumor specific accumulation *via* the EPR effect [47].

To confirm the ORM existence in PLGA-ORM NP formulations, FT-IR, DSC, and TGA studies were conducted (Fig. 2). In the FT-IR spectrum of PLGA NPs (Fig. 2A, **navy blue line**), intense peaks were found at 1741 cm−1, 1181 cm−1, and 1010 cm^{-1} due to C=O stretching of ester, C-O stretching of ester, and glycosidic (C–O–C/C–C/C–O) stretch vibrations. Because ORM has similar major functional groups in its structures (Fig 2A, **black line**), after encapsulation no additional peaks appeared in the FT-IR spectra of PLGA-ORM NPs (Fig. 2A, **red to magenta lines, upwards**). On the other hand, additional peaks were not attained in FT-IR after ORM encapsulation due to a higher degree of miscibility of ORM in the PLGA polymer matrix [48]. Yet, the bands produced by the PLGA polymer matrix may have masked ORM. This behavior was further confirmed with DSC analysis (Fig. 2B). DSC curves of pure PLGA NP formulation exhibit an endothermic peak at ~79°C (Fig. 2B, **black line**), indicative of the glass transition temperature of the formulation. Due to incorporation of ORM in the PLGA-ORM formulations, an exothermic peak appeared at ~58°C (Fig. 2B, **red to magenta lines, downwards**). Because of its superior blending of PLGA NPs and ORM in the PLGA-ORM NP formulations, PLGA glass transition peak disappeared or lowered the PLGA glass transition temperature. This indicates that ORM in nanoformulations is highly miscible. On the other hand, it appears that there is a significant reduction of crystallinity of the formulation. The presence of ORM in nanoformulations was

further confirmed by TGA (Fig. 2C). The significant weight loss of PLGA NPs begins at 250°C to 580°C (Fig. 2C, **black line**). This behavior is further accelerated due to the presence of ORM in PLGA-ORM nanoformulations (Fig. 2C, **red to magenta lines**). Weight loss of approximately 55% and 80% for PLGA NP formulations and 74% and 95% for PLGA-ORM NP formulations was observed at 350°C and 550°C, respectively. The greater weight loss is attributed to the presence of ORM in the nanoformulations.

3.2. Cellular uptake of PLGA-ORM NPs

Higher drug loading is an important index for a better drug delivery system. This is especially true for anti-cancer therapeutic drugs. The PLGA-ORM NPs were co-loaded with 6-coumarin (green fluorescence) to investigate the cellular uptake by confocal microscopy. As shown in Fig. 3, the coumarin-6-loaded PLGA-ORM NPs efficiently internalized and occupied different pockets of cell organelles within the HPAF-II cells. It was observed that coumarin-6-loaded PLGA-ORM NPs showed efficient cellular uptake (Fig. 3), indicated by high cytosolic staining and strong co-localization to the mitochondrial marker, mitotracker. Moreover, less co-localization of the NPs with early endosome and late endosome/lysosome markers indicate their escape from lysosomal degradation. Therefore, the results indicate that PLGA-ORM NPs are localized in the order of: mitochondria (Fig. 3, **C4**) > endosome (Fig. 3, **A4**) > lysosome (Fig. 3, **B4**). Therefore, higher accumulation of PLGA-ORM NPs was observed in cytosol (**green color, A2, B2, C2 in** Fig. 3) followed by mitochondria (Fig. 3, **C4**). This indicates that PLGA-ORM NPs are able to escape from late endosome and lysosome compartments and reach into the cytosol/mitochondria [49, 50] for efficient functioning rather than undergoing a lysosome recycling process. The specific reason for this phenomenon is that the anionic PLGA-ORM NPs convert to cationic in the acidic endo-lysosomal compartment, which leads the PLGA-ORM NPs to interact with the endo-lysosomal membrane and escape into the cytosol [51]. These results recognize PLGA-ORM NPs as effective drug delivery agents and prompted us to study their anti-cancer effects.

3.3. PLGA-ORM NPs inhibit proliferation and clonogenicity of pancreatic cancer cells

The cytotoxicity of PLGA-ORM NPs was evaluated in pancreatic cancer cell lines HPAF-II, BxPC-3, AsPC-1, Panc-1, and MiaPaca. PLGA-ORM NPs treatment inhibited the proliferation of pancreatic cancer cell lines in a dose dependent manner and with greater intensity as compared to free ORM (Fig. 4A). Further, both PLGA-ORM NPs and ORM treatment inhibited the clonogenic potential of pancreatic cancer cells as evident by the decreased number of colonies after treatment (Fig. 4B). This indicates that after incorporating ORM in the formulation, its anti-cancer activity is preserved.

3.4. PLGA-ORM NPs inhibit p-Akt and the downstream key proteins involved in pancreatic carcinogenesis

The Akt pathway is a potent survival signal in pancreatic cancer, as phosphorylation of Akt can facilitate cell survival and inactivate pro-apoptotic proteins [52]. Therefore, we sought to determine the effect of PLGA-ORM NPs and ORM treatments at 20 μM on the inhibition of Akt activation. Western blot analysis confirms that PLGA-ORM NPs treatment significantly decreases the phosphorylation of Akt levels compared to ORM (Fig. 5).

Interestingly, these treatments increased the levels of the phosphatase and tensin homologue deleted on chromosome ten (PTEN), which is a natural biological inhibitor of Akt in the PI3K-Akt pathway [52] (Fig. 5). Additionally, we observed a modulatory effect of treatment on the expression of two downstream cell cycle regulators, cyclin D1 and p27 [53] (Fig. 5). PLGA-ORM NP and ORM treatments both led to a two- or three-fold induction of cyclin D1 expression. Significant upregulation of $p27^{Kip1}$ expression by the treatment indicates that cells are inhibited from starting DNA synthesis [53, 54]. Akt represents a key signaling component in cell survival by activating downstream apoptotic proteins [55–57]. Upon treatment with PLGA-ORM NPs or ORM, pro-apoptotic protein Bax levels were increased while pro-survival protein survivin levels were decreased (Fig. 5). All these events favor induction of apoptosis, which was further confirmed by drastic activation of caspase-3 upon PLGA-ORM NPs and ORM treatments (Fig. 5) [42, 58]. This indicates that the PLGA-ORM NP formulation retains its biological activity and potency of ORM in order to mediate the anti-cancer effects.

3.5. PLGA-ORM NPs effectively inhibit pancreatic tumorigenesis in xenograft mice model

After evaluation of the retained potency and anti-cancer effects of the nanoparticle formulation of ORM *in vitro*, we validated its therapeutic relevance in a pancreatic cancer xenograft mice model. We used a subcutaneous (for solid tumor model) and intraperitoneal (for metastatic model) pre-clinical murine xenograft model generated with BxPC-3 cells. Intraperitoneal (*i.p.*) administration of PLGA-ORM NPs inhibited overall tumor burden as compared to control group that received PLGA alone (Fig. 6A). When compared to the control mice, mice treated with PLGA-ORM NPs ($p < 0.05$) showed a marked reduction in tumor weight (Fig. 6B) and tumor volume (Fig. 6C). Additionally, in the intraperitoneal model, tumors barely developed in the PLGA-ORM NP treated group. Upon further examination, we also found that there were very few metastases in the mice treated with PLGA-ORM NPs as compared to control (Fig. 6D, Table 1). Further, treatments of PLGA-ORM NPs also led to increased mice survival up to 60% (Fig. 6E). These data further confirm that PLGA-ORM NP treatment alone and along with gemcitabine could be an effective therapeutic modality for pancreatic cancer.

3.6. PLGA-ORM NP treatment alters expressions of proteins in xenograft tumors

To elucidate the putative mechanism of the anti-tumorigenic effects of PLGA-ORM NPs in mice, we analyzed the tumor tissues for changes in key oncogenic proteins that are known to be upregulated during pancreatic carcinogenesis, such as tumor associated mucin, MUC1 [41, 59]. The Western blot analysis of the total protein lysates isolated from tumor tissues indicated that the protein expression levels of MUC1 decreased in the mice treated with PLGA-ORM NPs (Fig. 6F). Additionally, the PLGA-ORM NPs treated tumors had decreased expression of HER2/neu oncogene that is often overexpressed in human pancreatic cancer specimens compared to normal pancreatic tissue [60] (Fig. 6F). Similar results were found on analysis of formalin fixed paraffin embedded (FFPE) tissue sections through tumor histopathology and immunohistochemical (IHC) analyses that showed less staining of MUC1 and HER2/neu, indicative of their low expression (Fig. 7A). We observed a clear inhibition of CD31 expression in tumor tissues from mice treated with PLGA-ORM NPs through Western blotting (Fig. 6F).

The stained tissues showed that the microvessel density (CD31 expression) in PLGA-ORM NPs treated tumors was much less than with control treatments. Further, the tissues from control groups had larger sized vessels as compared to the ones treated with PLGA-ORM NPs (Fig. 7B). These results suggest that PLGA-ORM NPs may have an anti-angiogenesis function as observed in this animal model. Additionally, in accordance with the *in vitro* results, the PLGA-ORM NPs treated tumor tissues were stained for less p-Akt expression, which further confirmed the involvement of the p-Akt pathway in PLGA-ORM NPs induced pancreatic tumor growth inhibition (Fig. 6F). Moreover, PLGA-ORM NPs also inhibited the expression of proliferating cell nuclear antigen (PCNA) and cytokeratin 19 (duct epithelial marker) (Fig. 7B) that are found in a vast majority of pancreatic adenocarcinomas [61], indicative of a decrease in proliferation of pancreatic cancer cells.

4. Discussion

Pancreatic cancer has continued to carry a dismal prognosis while other cancers have shown significant improvements in overall survival during the past several decades [62]. Understandings of PDAC genetics and biology [63–65] have led to the development of current therapeutic strategies, but their application has failed to improve clinical outcomes of pancreatic cancer patients [66–68]. One of the main reasons for this is insufficient drug accumulation at the tumor site of the pancreas, a relatively small organ tucked away in a corner of the digestive tract with high desmoplasia. Furthermore, repetitive use of such potent anti-cancer drugs not only induces significant systemic toxicity but also chemo-resistance. Therefore, the challenge is to identify a molecule with a higher therapeutic index, low systemic toxicity, and that can tackle major oncogenic signaling pathways operating in pancreatic tumors. Ormeloxifene is a synthetic molecule that is widely used as an oral contraceptive in humans, and exhibits potent anti-cancer activity by targeting the key underlying oncogenic molecular mechanisms [18–25]. Hence, our aim of this study was to enhance ORM delivery at the tumor site for improved therapeutic effects/index for pancreatic cancer treatment. To this end, we have developed an efficient PLGA NP (PLGA-ORM NP) based delivery system, to enhance the anti-cancer efficiency of ORM at the tumor site.

In the present study, an optimized PLGA-ORM20 NP formulation was made with an average particle size of 101.4 ± 1.5 nm (Fig. 1) with 84.96 ± 4.75% drug-loading capacity. The release profile of ORM from PLGA-ORM 20 is presented in Figure S1 (Supplementary Information I). The release of ORM is relatively rapid at 1–6 h and thereafter the release pattern is gradual and sustained. This formulation provides good suspension while maintaining long-term stability, up to 6 months. From the results of FT-IR, DSC, and TGA (Fig. 2), it is evident that PLGA, PVA, and PLL polymers form undefined structure in PLGA-ORM NPs, which allow for the controlled release in cancer cells. We observed that PLGA-ORM NPs delivered a higher payload of ORM in pancreatic cancer cells (Fig. 3), which was correlated with increased cytotoxicity in pancreatic cancer cells (Fig. 4).

Elucidating the internalization mechanisms could provide crucial insights into engineering novel cancer therapeutics yielding more potent and selective nanoformulations. The uptake and internalization of PLGA-ORM NPs follow an endocytotic pathway, which is consistent

with most of the conventional nanoformulations [69]. It was observed that PLGA-ORM NPs are able to escape from late endosome and lysosome compartments and reach into the cytosol/mitochondria (Fig. 3). This is evident from the residence of PLGA-ORM NPs in cytosol compartments and the release of loaded drug molecules in active form, causing superior activity. The subsequent intracellular trafficking studies were based on inferences from *in vitro* biological assays.

In this study the PLGA-ORM NPs demonstrated enhanced anti-cancer effects over free ORM against a panel of five pancreatic cancer cell lines in proliferation and clonogenic potential assays (Fig. 4). Additionally, our investigation also suggests that the PLGA-ORM NPs target Akt phosphorylation regulating the downstream associated proteins (cyclin D1, p27, Bax, survivin, and caspase-3) and induces pancreatic cancer cell death (Fig. 5). These results were consistent with the *in vivo* findings of a xenograft mouse model, confirming the role of Akt signaling in the PLGA-ORM NPs induced anti-cancer effects (Fig. 6). Inhibition of Akt phosphorylation has been shown to sensitize these cells to the apoptotic effect of chemotherapy [70–72]. Loss of PTEN protein is an important event and has been observed to be inversely correlated with Akt phosphorylation [73]. The increased PTEN expression in pancreatic cancer cells on PLGA-ORM NP treatment suggests that PLGA-ORM NPs induced an increase in PTEN expression that leads to the inhibition of Akt phosphorylation. Additionally, PLGA-ORM NPs treatment efficiently altered the expression profiles of key associated proteins in pancreatic xenograft tumors to efficaciously decrease pancreatic tumor growth in mice (Fig. 6). Interestingly, this included the downregulation of important proteins, MUC1 and HER2, which have a major role in pancreatic cancer development and progression (Fig. 6 **and** 7). MUC1 is associated with cellular transformation and tumorigenicity and is considered to be an important tumor-associated antigen (TAA) for cancer therapy [59]. Furthermore, HER2 is also involved in increasing pancreatic tumor growth and aggressiveness [41] and is largely associated with poor prognosis. Other important observations include the decreased CD31 expression and microvessel density in the PLGA-ORM NPs treated mouse tumors that suggest inhibition of tumor vascularization leading to efficient drug internalization in tumors (Fig. 6 **and** 8). Additionally, the reduced staining of the proliferating cell nuclear antigen (PCNA) and cytokeratin-19 in pancreatic tumors clearly indicates that PLGA-ORM NPs inhibit the proliferation of pancreatic tumor cells. Altogether, these results signify that PLGA-ORM NPs are capable of delivering ORM efficiently to the tumor cells to control the key oncogenes driving oncogenic signaling pathways, such as MUC1, HER2, and p-Akt, as well as biological events, which can play a vital role in pancreatic cancer therapeutics (Fig. 6 **and** 7).

From a clinical translational point of view, achieving the highest drug loading is more favorable to improve pharmacokinetic profiles. Therefore, we have engineered an optimized PLGA-ORM20 NP formulation with higher loading capacity. The higher drug loading not only minimizes (i) processing, (ii) overall raw materials, and (iii) non-active ingredients for generating the formulation, but delivers an equivalent dose of ORM efficiently. Overall, in this proof-of-concept study, we have demonstrated that the PLGA-ORM20 NP formulation is highly suitable to deliver ORM more efficiently at the tumor site to induce superior anti-cancer activity (Fig 8). To further improve its targeted delivery to pancreatic cancer cells/

tumors, we are in the process of developing a mucin-targeted PLGA-ORM NP formulation by conjugating with an anti-MUC1 MAb and/or anti-MUC13 MAb. These targeted NPs can be used both for therapy and diagnostic (theranostic) applications for pancreatic cancer.

5. Conclusion

Nanoparticle based drug delivery technologies provide a successful therapeutic platform for targeted cancer therapeutics. In this study, we have developed an optimized PLGA-ORM NP formulation for efficient delivery of ORM to pancreatic cancer. Our findings demonstrate that PLGA-ORM NPs have superior dose-dependent, anti-proliferative, and clonogenic effects on human pancreatic cancer cell lines compared to free ormeloxifene. These particles efficiently escape from endosome/lysosome and accumulate in cytosol to induce such improved anti-cancer activity in cancer cells. *In vitro* studies suggest that PLGA-ORM NPs significantly inhibit p-Akt and the downstream key proteins involved in pancreatic cancer progression. Further, PLGA-ORM NPs are able to reach the tumors through EPR, resulting in reduction of tumor growth and metastatic lesions in a mouse model. Additionally, PLGA-ORM NPs treated tumors demonstrated downregulation of key oncogenic proteins that are known to be involved in pancreatic cancer development and progression. Altogether, these results indicated that the PLGA-ORM NPs may have great potential for pancreatic cancer treatment.

Supplementary Material

Refer to Web version on PubMed Central for supplementary material.

Acknowledgments

This work was partially supported by the National Institutes of Health (R01 CA142736 to SCC and U01 CA162106 to SCC and MJ), and the Department of Defense (PC130870 to SCC and MJ). The authors thank the Imaging, Molecular Pathology, Flow Cytometry and Tumor Biology Cores at Sanford Research (P20 GM103548-02 to Dr. KM Miskimins) and the UTHSC Tissue Services Core for tissue section, staining, and imaging. We gratefully acknowledge Cathy Christopherson (Sanford Research) for editorial assistance.

References

1. Siegel R, Naishadham D, Jemal A. Cancer statistics, 2013. CA Cancer J Clin. 2013; 63:11–30. [PubMed: 23335087]
2. Long J, Zhang Y, Yu X, Yang J, LeBrun DG, Chen C, et al. Overcoming drug resistance in pancreatic cancer. Expert Opin Ther Targets. 2011; 15:817–828. [PubMed: 21391891]
3. American Cancer Society (ACS) Cancer Facts & Figures. Atlanta: American Cancer Society; 2013.
4. Di Marco M, Di Cicilia R, Macchini M, Nobili E, Vecchiarelli S, Brandi G, et al. Metastatic pancreatic cancer: is gemcitabine still the best standard treatment? (Review). Oncol Rep. 2010; 23:1183–1192. [PubMed: 20372829]
5. Kleynberg RL, Sofi AA, Chaudhary RT. Hand-foot hyperpigmentation skin lesions associated with combination gemcitabine-carboplatin (GemCarbo) therapy. Am J Ther. 2011; 18:e261–e263. [PubMed: 20460984]
6. Pedersen AG. Phase I studies of gemcitabine combined with carboplatin or paclitaxel. Semin Oncol. 1997; 24:S7–S64. S7–S8. [PubMed: 9194483]
7. Rapoport N, Kennedy AM, Shea JE, Scaife CL, Nam KH. Ultrasonic nanotherapy of pancreatic cancer: lessons from ultrasound imaging. Mol Pharm. 2010; 7:22–31. [PubMed: 19899813]

8. Yallapu MM, Ebeling MC, Khan S, Sundram V, Chauhan N, Gupta BK, et al. Novel curcumin-loaded magnetic nanoparticles for pancreatic cancer treatment. Mol Cancer Ther. 2013; 12:1471–1480. [PubMed: 23704793]
9. Issa NT, Byers SW, Dakshanamurthy S. Drug repurposing: translational pharmacology, chemistry, computers and the clinic. Curr Top Med Chem. 2013; 13:2328–2336. [PubMed: 24059462]
10. Cragg GM, Grothaus PG, Newman DJ. New horizons for old drugs and drug leads. J Nat Prod. 2014; 77:703–723. [PubMed: 24499205]
11. Foretz M, Guigas B, Bertrand L, Pollak M, Viollet B. Metformin: From Mechanisms of Action to Therapies. Cell Metab. 2014; 20:953–966. [PubMed: 25456737]
12. Kasznicki J, Sliwinska A, Drzewoski J. Metformin in cancer prevention and therapy. Ann Transl Med. 2014; 2:57. [PubMed: 25333032]
13. Aldea M, Craciun L, Tomuleasa C, Berindan-Neagoe I, Kacso G, Florian IS, et al. Repositioning metformin in cancer: genetics, drug targets, and new ways of delivery. Tumour Biol. 2014; 35:5101–5110. [PubMed: 24504677]
14. Bansode FW, Chauhan SC, Makker A, Singh MM. Uterine luminal epithelial alkaline phosphatase activity and pinopod development in relation to endometrial sensitivity in the rat. Contraception. 1998; 58:61–68. [PubMed: 9743898]
15. Kamboj VP, Setty BS, Chandra H, Roy SK, Kar AB. Biological profile of Centchroman--a new post-coital contraceptive. Indian J Exp Biol. 1977; 15:1144–1150. [PubMed: 96021]
16. Gara RK, Sundram V, Chauhan SC, Jaggi M. Anti-cancer potential of a novel SERM ormeloxifene. Curr Med Chem. 2013; 20:4177–4184. [PubMed: 23895678]
17. Giri AK, Mukhopadhyay A, Sun J, Hsie AW, Ray S. Antimutagenic effects of centchroman--a contraceptive and a candidate drug for breast cancer in multiple mutational assays. Mutagenesis. 1999; 14:613–620. [PubMed: 10567037]
18. Misra NC, Nigam PK, Gupta R, Agarwal AK, Kamboj VP. Centchroman--a non-steroidal anti-cancer agent for advanced breast cancer: phase-II study. Int J Cancer. 1989; 43:781–783. [PubMed: 2714882]
19. Maher DM, Khan S, Nordquist JL, Ebeling MC, Bauer NA, Kopel L, et al. Ormeloxifene efficiently inhibits ovarian cancer growth. Cancer Lett. 2014
20. Mishra R, Tiwari A, Bhadauria S, Mishra J, Murthy PK, Murthy PS. Therapeutic effect of centchroman alone and in combination with glycine soya on 7,12-dimethylbenz[alpha]anthracene-induced breast tumor in rat. Food Chem Toxicol. 2010; 48:1587–1591. [PubMed: 20332012]
21. Nigam M, Ranjan V, Srivastava S, Sharma R, Balapure AK. Centchroman induces G0/G1 arrest and caspase-dependent apoptosis involving mitochondrial membrane depolarization in MCF-7 and MDA MB-231 human breast cancer cells. Life Sci. 2008; 82:577–590. [PubMed: 18279897]
22. Nigam M, Singh N, Ranjan V, Zaidi D, Sharma R, Nigam D, et al. Centchroman mediated apoptosis involves cross-talk between extrinsic/intrinsic pathways and oxidative regulation. Life Sci. 2010; 87:750–758. [PubMed: 21034746]
23. Pal P, Kanaujiya JK, Lochab S, Tripathi SB, Bhatt ML, Singh PK, et al. 2-D gel electrophoresis-based proteomic analysis reveals that ormeloxifen induces G0-G1 growth arrest and ERK-mediated apoptosis in chronic myeloid leukemia cells K562. Proteomics. 2011; 11:1517–1529. [PubMed: 21360677]
24. Srivastava VK, Gara RK, Bhatt ML, Sahu DP, Mishra DP. Centchroman inhibits proliferation of head and neck cancer cells through the modulation of PI3K/mTOR pathway. Biochem Biophys Res Commun. 2011; 404:40–45. [PubMed: 21094138]
25. Singh MM. Centchroman, a selective estrogen receptor modulator, as a contraceptive and for the management of hormone-related clinical disorders. Med Res Rev. 2001; 21:302–347. [PubMed: 11410933]
26. Pries AR, Hopfner M, le Noble F, Dewhirst MW, Secomb TW. The shunt problem: control of functional shunting in normal and tumour vasculature. Nat Rev Cancer. 2010; 10:587–593. [PubMed: 20631803]
27. Provenzano PP, Cuevas C, Chang AE, Goel VK, Von Hoff DD, Hingorani SR. Enzymatic targeting of the stroma ablates physical barriers to treatment of pancreatic ductal adenocarcinoma. Cancer Cell. 2012; 21:418–429. [PubMed: 22439937]

28. Stylianopoulos T, Martin JD, Chauhan VP, Jain SR, Diop-Frimpong B, Bardeesy N, et al. Causes, consequences, and remedies for growth-induced solid stress in murine and human tumors. Proc Natl Acad Sci U S A. 2012; 109:15101–15108. [PubMed: 22932871]
29. Neesse A, Michl P, Frese KK, Feig C, Cook N, Jacobetz MA, et al. Stromal biology and therapy in pancreatic cancer. Gut. 2011; 60:861–868. [PubMed: 20966025]
30. Farrell JJ, Elsaleh H, Garcia M, Lai R, Ammar A, Regine WF, et al. Human equilibrative nucleoside transporter 1 levels predict response to gemcitabine in patients with pancreatic cancer. Gastroenterology. 2009; 136:187–195. [PubMed: 18992248]
31. Jain RK. Transport of molecules across tumor vasculature. Cancer Metastasis Rev. 1987; 6:559–593. [PubMed: 3327633]
32. Hobbs SK, Monsky WL, Yuan F, Roberts WG, Griffith L, Torchilin VP, et al. Regulation of transport pathways in tumor vessels: role of tumor type and microenvironment. Proc Natl Acad Sci U S A. 1998; 95:4607–4612. [PubMed: 9539785]
33. Shubik P. Vascularization of tumors: a review. J Cancer Res Clin Oncol. 1982; 103:211–226. [PubMed: 6181069]
34. Dinarvand R, Sepehri N, Manoochehri S, Rouhani H, Atyabi F. Polylactide-co-glycolide nanoparticles for controlled delivery of anticancer agents. Int J Nanomedicine. 2011; 6:877–895. [PubMed: 21720501]
35. Danhier F, Ansorena E, Silva JM, Coco R, Le Breton A, Preat V. PLGA-based nanoparticles: an overview of biomedical applications. J Control Release. 2012; 161:505–522. [PubMed: 22353619]
36. Yallapu MM, Gupta BK, Jaggi M, Chauhan SC. Fabrication of curcumin encapsulated PLGA nanoparticles for improved therapeutic effects in metastatic cancer cells. J Colloid Interface Sci. 2010; 351:19–29. [PubMed: 20627257]
37. Yallapu MM, Khan S, Maher DM, Ebeling MC, Sundram V, Chauhan N, et al. Anti-cancer activity of curcumin loaded nanoparticles in prostate cancer. Biomaterials. 2014; 35:8635–8648. [PubMed: 25028336]
38. Yallapu MM, Maher DM, Sundram V, Bell MC, Jaggi M, Chauhan SC. Curcumin induces chemo/radio-sensitization in ovarian cancer cells and curcumin nanoparticles inhibit ovarian cancer cell growth. J Ovarian Res. 2010; 3:11. [PubMed: 20429876]
39. Kumar P, Sreeramulu J. A Stability-indicating Reversed-Phase High Performance Liquid Chromatography Method for Simultaneous determination of Ormeloxifene in Pure and Pharmaceutical Formulation. Int J Chem Tech Res. 2011; 3:314–320.
40. Barltrop JA, Owen TC, Cory AH, Cory JG. 5-(3-carboxymethoxyphenyl)-2-(4,5-dimethylthiazolyl)-3-(4-sulfophenyl)tetrazolium, inner salt (MTS) and related analogs of 3-(4,5-dimethylthiazolyl)-2,5-diphenyltetrazolium bromide (MTT) reducing to purple water-soluble formazans As cell-viability indicators. Bioorganic & Medicinal Chemistry Letters. 1991; 1:611–614.
41. Chauhan SC, Ebeling MC, Maher DM, Koch MD, Watanabe A, Aburatani H, et al. MUC13 mucin augments pancreatic tumorigenesis. Mol Cancer Ther. 2012; 11:24–33. [PubMed: 22027689]
42. Khan S, Kaur R, Shah BA, Malik F, Kumar A, Bhushan S, et al. A Novel cyano derivative of 11-Keto-beta-Boswellic acid causes apoptotic death by disrupting PI3K/AKT/Hsp-90 cascade, mitochondrial integrity, and other cell survival signaling events in HL-60 cells. Mol Carcinog. 2012; 51:679–695. [PubMed: 21751262]
43. Chauhan SC, Vannatta K, Ebeling MC, Vinayek N, Watanabe A, Pandey KK, et al. Expression and functions of transmembrane mucin MUC13 in ovarian cancer. Cancer Res. 2009; 69:765–774. [PubMed: 19176398]
44. Khan S, Ebeling MC, Zaman MS, Sikander M, Yallapu MM, Chauhan N, et al. MicroRNA-145 targets MUC13 and suppresses growth and invasion of pancreatic cancer. Oncotarget. 2014; 5:7599–7609. [PubMed: 25277192]
45. Bertrand N, Wu J, Xu X, Kamaly N, Farokhzad OC. Cancer nanotechnology: the impact of passive and active targeting in the era of modern cancer biology. Adv Drug Deliv Rev. 2014; 66:2–25. [PubMed: 24270007]
46. Acharya S, Sahoo SK. PLGA nanoparticles containing various anticancer agents and tumour delivery by EPR effect. Adv Drug Deliv Rev. 2011; 63:170–183. [PubMed: 20965219]

47. Peer D, Karp JM, Hong S, Farokhzad OC, Margalit R, Langer R. Nanocarriers as an emerging platform for cancer therapy. Nat Nanotech. 2007; 2:751–760.
48. Martins KF, Messias AD, Leite FL, Duek EAR. Preparation and characterization of paclitaxel-loaded PLDLA microspheres. Mater Res. 2014; 17:650–656.
49. Weissig V, Boddapati SV, Jabr L, D'Souza GG. Mitochondria-specific nanotechnology. Nanomedicine (Lond). 2007; 2:275–285. [PubMed: 17716174]
50. Han M, Kickhoefer VA, Nemerow GR, Rome LH. Targeted vault nanoparticles engineered with an endosomolytic peptide deliver biomolecules to the cytoplasm. ACS Nano. 2011; 5:6128–6137. [PubMed: 21740042]
51. Panariti A, Miserocchi G, Rivolta I. The effect of nanoparticle uptake on cellular behavior: disrupting or enabling functions? Nanotechnol Sci Appl. 2012; 5:87–100. [PubMed: 24198499]
52. Schlieman MG, Fahy BN, Ramsamooj R, Beckett L, Bold RJ. Incidence, mechanism and prognostic value of activated AKT in pancreas cancer. Br J Cancer. 2003; 89:2110–2115. [PubMed: 14647146]
53. Mirza AM, Gysin S, Malek N, Nakayama K, Roberts JM, McMahon M. Cooperative regulation of the cell division cycle by the protein kinases RAF and AKT. Mol Cell Biol. 2004; 24:10868–10881. [PubMed: 15572689]
54. Hodul PJ, Dong Y, Husain K, Pimiento JM, Chen J, Zhang A, et al. Vitamin E delta-tocotrienol induces p27(Kip1)-dependent cell-cycle arrest in pancreatic cancer cells via an E2F-1-dependent mechanism. PLoS One. 2013; 8:e52526. [PubMed: 23393547]
55. Datta SR, Dudek H, Tao X, Masters S, Fu H, Gotoh Y, et al. Akt phosphorylation of BAD couples survival signals to the cell-intrinsic death machinery. Cell. 1997; 91:231–241. [PubMed: 9346240]
56. del Peso L, Gonzalez-Garcia M, Page C, Herrera R, Nunez G. Interleukin-3-induced phosphorylation of BAD through the protein kinase Akt. Science. 1997; 278:687–689. [PubMed: 9381178]
57. Scheid MP, Woodgett JR. Unravelling the activation mechanisms of protein kinase B/Akt. FEBS Lett. 2003; 546:108–112. [PubMed: 12829245]
58. Khan S, Chib R, Shah BA, Wani ZA, Dhar N, Mondhe DM, et al. A cyano analogue of boswellic acid induces crosstalk between p53/PUMA/Bax and telomerase that stages the human papillomavirus type 18 positive HeLa cells to apoptotic death. Eur J Pharmacol. 2011; 660:241–248. [PubMed: 21440536]
59. Wang L, Chen H, Pourgholami MH, Beretov J, Hao J, Chao H, et al. Anti-MUC1 monoclonal antibody (C595) and docetaxel markedly reduce tumor burden and ascites, and prolong survival in an in vivo ovarian cancer model. PLoS One. 2011; 6:e24405. [PubMed: 21931707]
60. Buchler P, Reber HA, Eibl G, Roth MA, Buchler MW, Friess H, et al. Combination therapy for advanced pancreatic cancer using Herceptin plus chemotherapy. Int J Oncol. 2005; 27:1125–1130. [PubMed: 16142331]
61. Jain R, Fischer S, Serra S, Chetty R. The use of Cytokeratin 19 (CK19) immunohistochemistry in lesions of the pancreas, gastrointestinal tract, and liver. Appl Immunohistochem Mol Morphol. 2010; 18:9–15. [PubMed: 19956064]
62. Li D, Xie K, Wolff R, Abbruzzese JL. Pancreatic cancer. Lancet. 2004; 363:1049–1057. [PubMed: 15051286]
63. Penchev VR, Rasheed ZA, Maitra A, Matsui W. Heterogeneity and targeting of pancreatic cancer stem cells. Clin Cancer Res. 2012; 18:4277–4284. [PubMed: 22896694]
64. Nagaraju GP, El-Rayes BF. SPARC and DNA methylation: possible diagnostic and therapeutic implications in gastrointestinal cancers. Cancer Lett. 2013; 328:10–17. [PubMed: 22939997]
65. Olive KP, Jacobetz MA, Davidson CJ, Gopinathan A, McIntyre D, Honess D, et al. Inhibition of Hedgehog signaling enhances delivery of chemotherapy in a mouse model of pancreatic cancer. Science. 2009; 324:1457–1461. [PubMed: 19460966]
66. Crane CH, Iacobuzio-Donahue CA. Keys to personalized care in pancreatic oncology. J Clin Oncol. 2012; 30:4049–4050. [PubMed: 23045599]
67. Kindler HL, Ioka T, Richel DJ, Bennouna J, Letourneau R, Okusaka T, et al. Axitinib plus gemcitabine versus placebo plus gemcitabine in patients with advanced pancreatic

adenocarcinoma: a double-blind randomised phase 3 study. Lancet Oncol. 2011; 12:256–262. [PubMed: 21306953]

68. Schmidt J, Abel U, Debus J, Harig S, Hoffmann K, Herrmann T, et al. Open-label, multicenter, randomized phase III trial of adjuvant chemoradiation plus interferon Alfa-2b versus fluorouracil and folinic acid for patients with resected pancreatic adenocarcinoma. J Clin Oncol. 2012; 30:4077–4083. [PubMed: 23008325]
69. Paillard A, Hindre F, Vignes-Colombeix C, Benoit JP, Garcion E. The importance of endo-lysosomal escape with lipid nanocapsules for drug subcellular bioavailability. Biomaterials. 2010; 31:7542–7554. [PubMed: 20630585]
70. Ng SSW, Tsao MS, Chow S, Hedley DW. Inhibition of phosphatidylinositide 3-kinase enhances gemcitabine-induced apoptosis in human pancreatic cancer cells. Cancer Res. 2000; 60:5451–5455. [PubMed: 11034087]
71. Perugini RA, McDade TP, Vittimberga FJ Jr, Callery MP. Pancreatic cancer cell proliferation is phosphatidylinositol 3-kinase dependent. J Surg Res. 2000; 90:39–44. [PubMed: 10781373]
72. Yao Z, Okabayashi Y, Yutsudo Y, Kitamura T, Ogawa W, Kasuga M. Role of Akt in growth and survival of PANC-1 pancreatic cancer cells. Pancreas. 2002; 24:42–46. [PubMed: 11741181]
73. Ma J, Sawai H, Matsuo Y, Ochi N, Yasuda A, Takahashi H, et al. IGF-1 mediates PTEN suppression and enhances cell invasion and proliferation via activation of the IGF-1/PI3K/Akt signaling pathway in pancreatic cancer cells. J Surg Res. 2010; 160:90–101. [PubMed: 19560785]

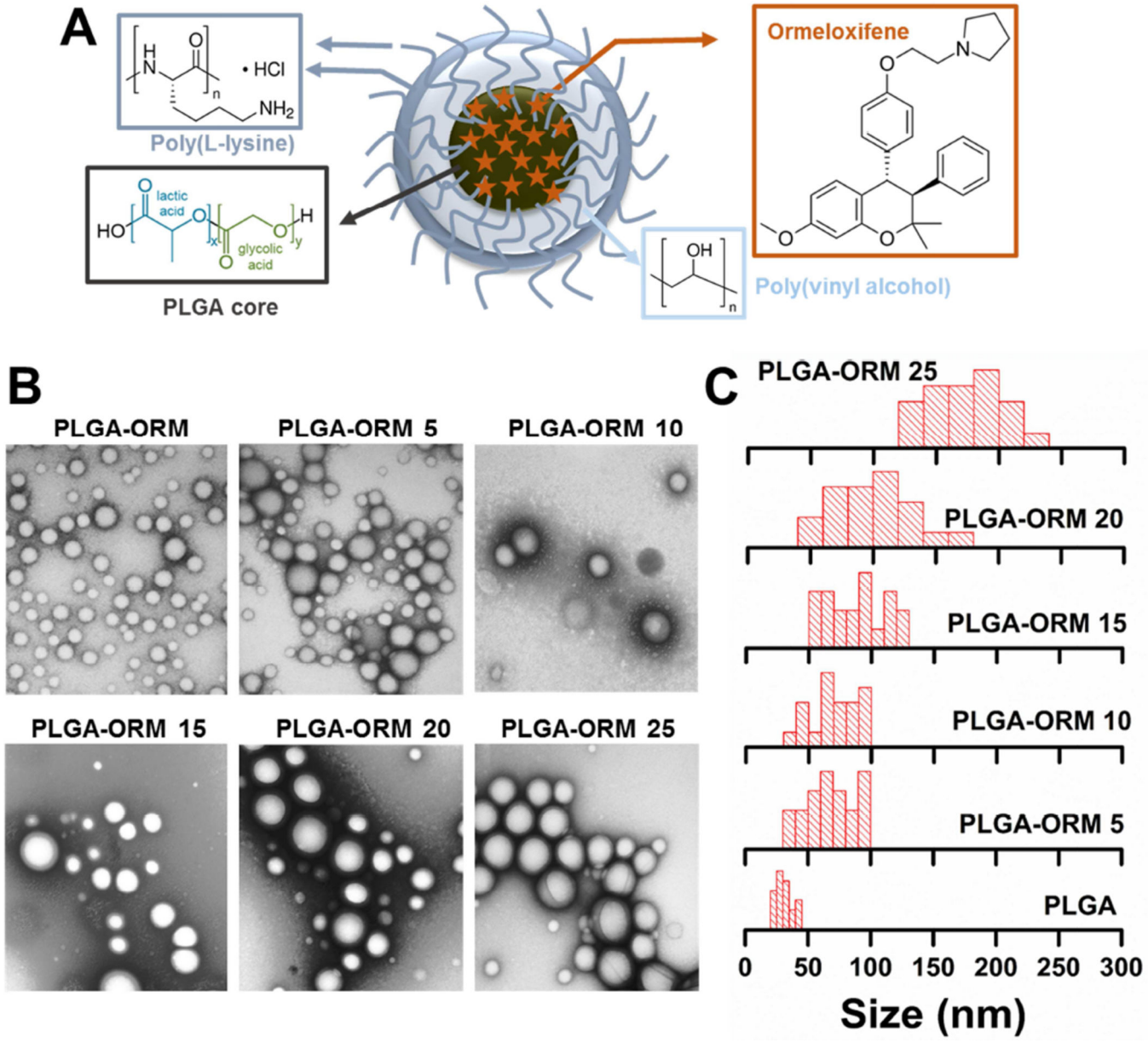

Figure 1. Preparation of PLGA-ORM NP formulations

(A). Schematic showing ORM encapsulation in PLGA-based NPs (PLGA-ORM NPs) prepared using a nano-precipitation technique. **(B).** Representative TEM images of PLGA and PLGA-ORM NPs. Scale bars on TEM images equal 200 nm. **(C).** Evaluation of nanoparticle size from TEM images using ImageJ software. Data represents an average of at least 20 particles in two different fields of view in TEM images.

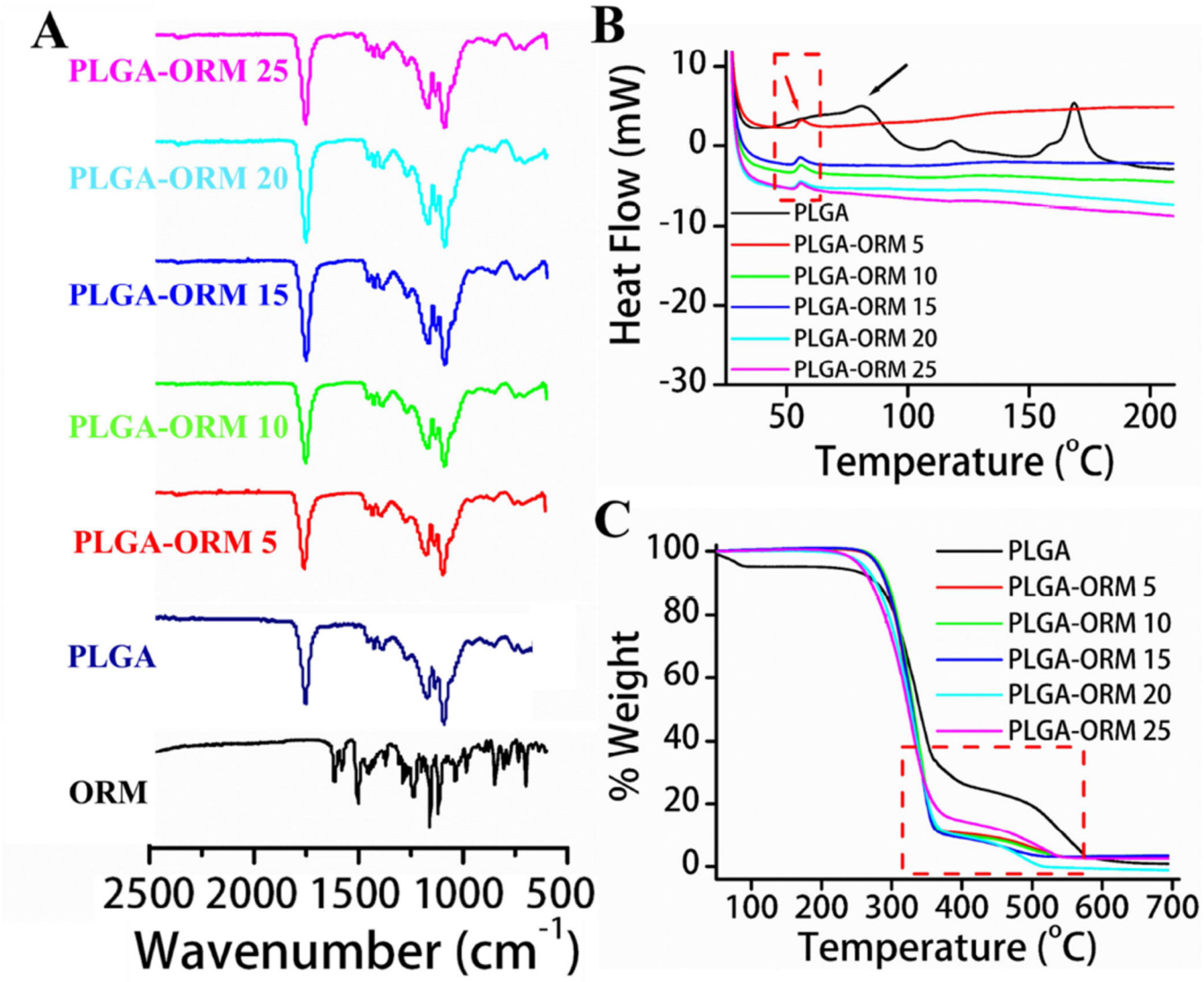

Figure 2. Characterization of PLGA-ORM NP formulations

(A). FT-IR spectra of ORM, PLGA NPs and PLGA-ORM NP formulations. **(B).** DSC endothermic curves of PLGA and PLGA-ORM NP nanoformulations. **(C).** Thermogravimetric weight loss curves of PLGA and PLGA-ORM NP nanoformulations. Note: All these characterization suggest ORM incorporation in the PLGA-ORM NP formulation.

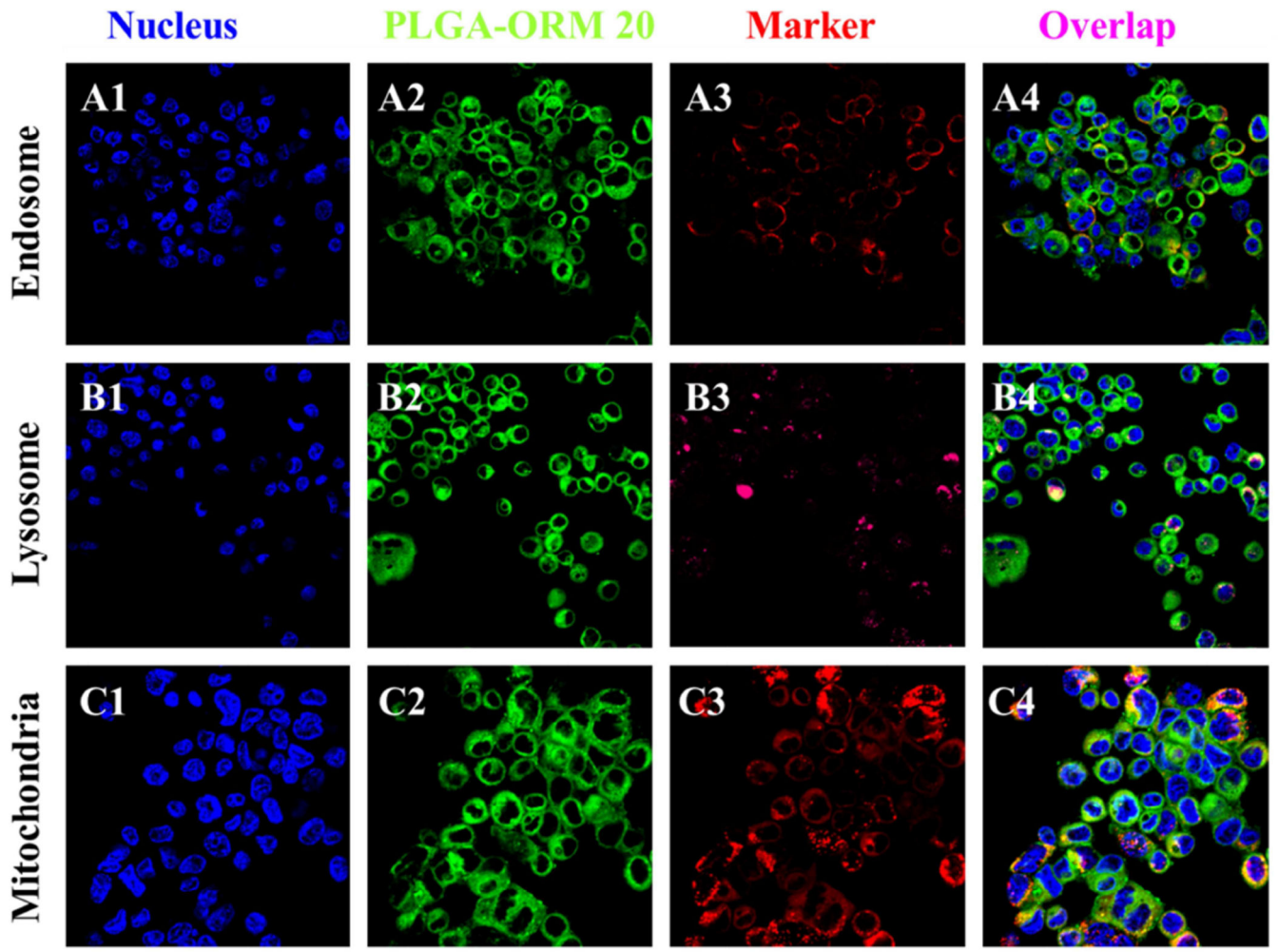

Figure 3. Fate and subcellular localization of 6-coumarin labelled PLGA-ORM 20 nanoformulation

HPAF-II PanCa cells (1×10^5/well) were exposed to 50 μg 6-coumarin labelled PLGA-ORM 20 NPs for 6 hrs, cells were washed twice with PBS, fixed in 2% paraformaldehyde for 10 min, and permeabilized with 0.1% TritonX-100 in PBS for 10 min. For co-localization evaluation, CellLight® Late Endosomes-RFP, LysoTracker Red, and Mito Tracker Red, were used to stain as a marker for endosome, lysosome, and mitochondria, respectively. DAPI was used to stain nuclei. Green color represents uptake of 6-coumarin labelled PLGA-ORM 20 formulation and purple color indicates co-localization of 6-coumarin labelled PLGA-ORM 20 NPs in endosome/lysosome/mitochondria. (Original Magnifications 600×)

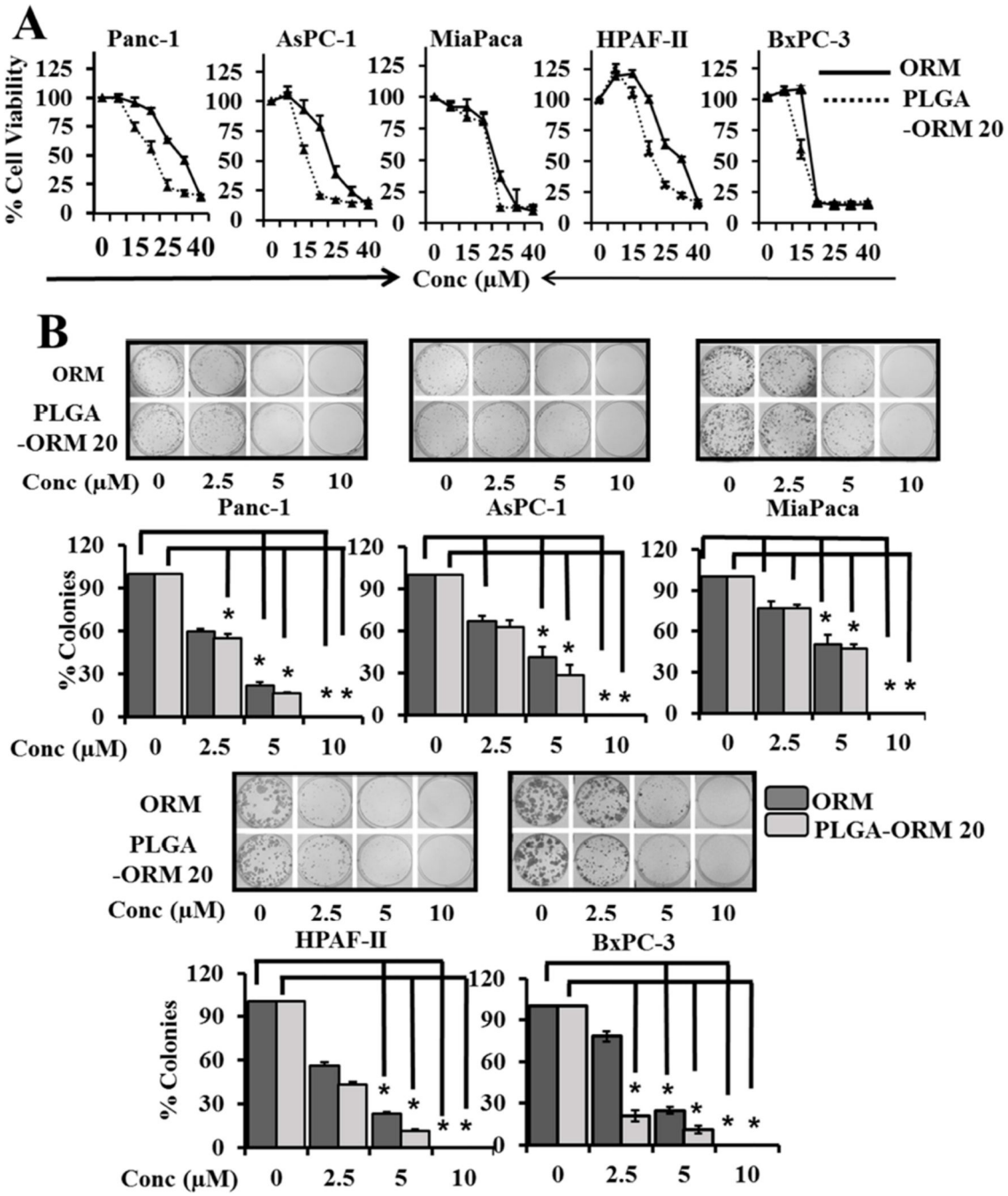

Figure 4. ORM and PLGA-ORM NPs inhibit proliferation and colonogenicity of PanCa cells

(A). Effect of ORM and PLGA-ORM NPs on cell growth. PanCa cells (5×10^3/well in 96-well plate) were treated with 0–40 μM ORM or PLGA-ORM 20 formulation or respective control for 48 h. The proliferation of cells was assessed by MTS assay. Data is shown as percentage with respect to un-treated cells. **(B).** Colonogenicity assay was performed for the ability of cells to form colonies (percent inhibition) following 0–10 μM ORM or PLGA-ORM 20 treatment for 2 weeks. Cells were photographed and counted using an imaging system. Bars represent mean ± SD; n=3; *p<0.05

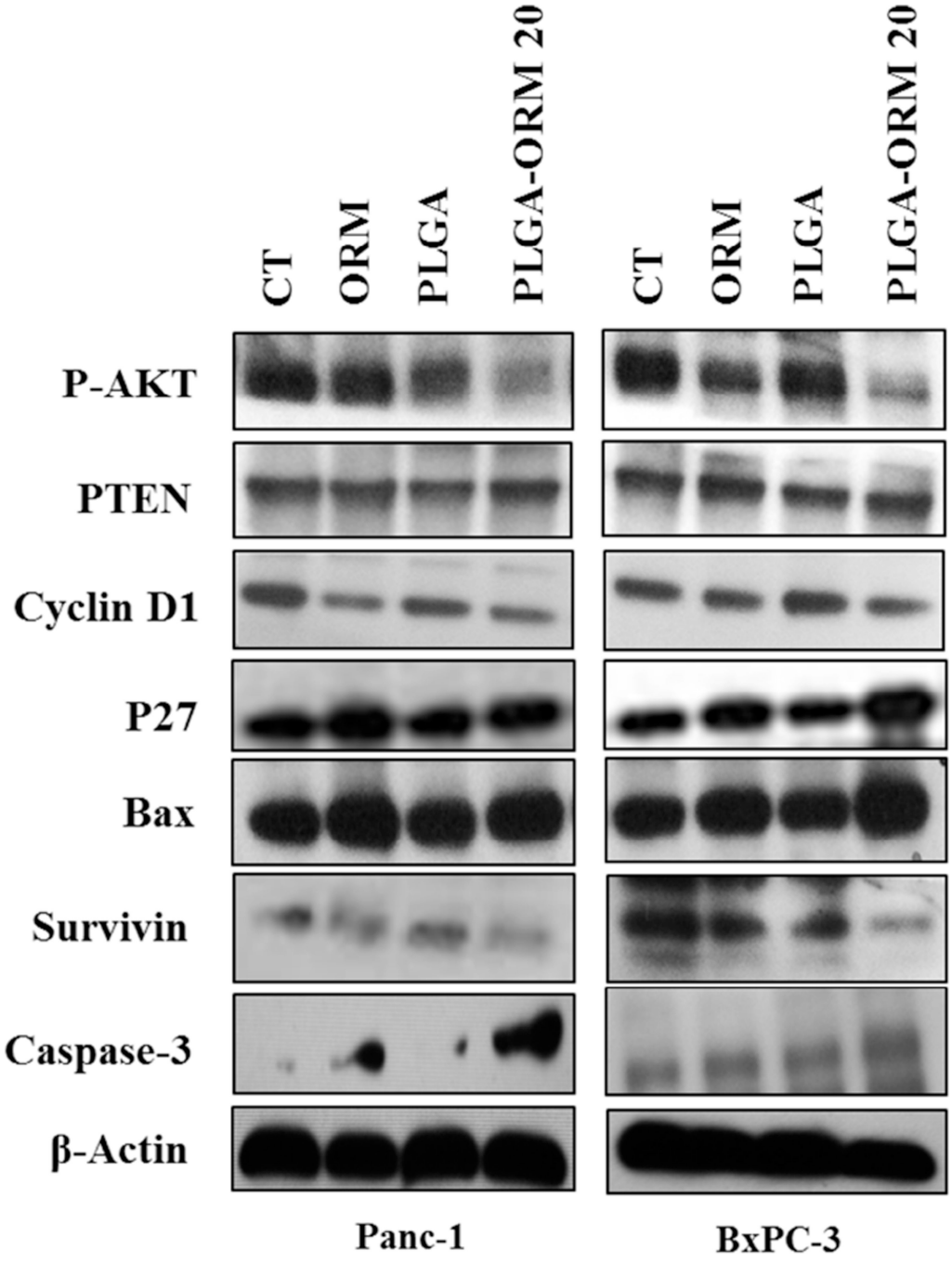

Figure 5. PLGA-ORM NPs inhibit p-AKT and the downstream key proteins associated with pancreatic carcinogenesis

HPAF-II and BxPC-3 PanCa cells were treated with 20 μM ORM or PLGA-ORM 20 or their respective controls, for 48 h, and the cell lysates were collected and immunoblotted for p-Akt, PTEN, cyclin D1, p27, Bax, survivin, caspase-3, and β-actin (loading control). The results were consistent in two independent sets of experiments.

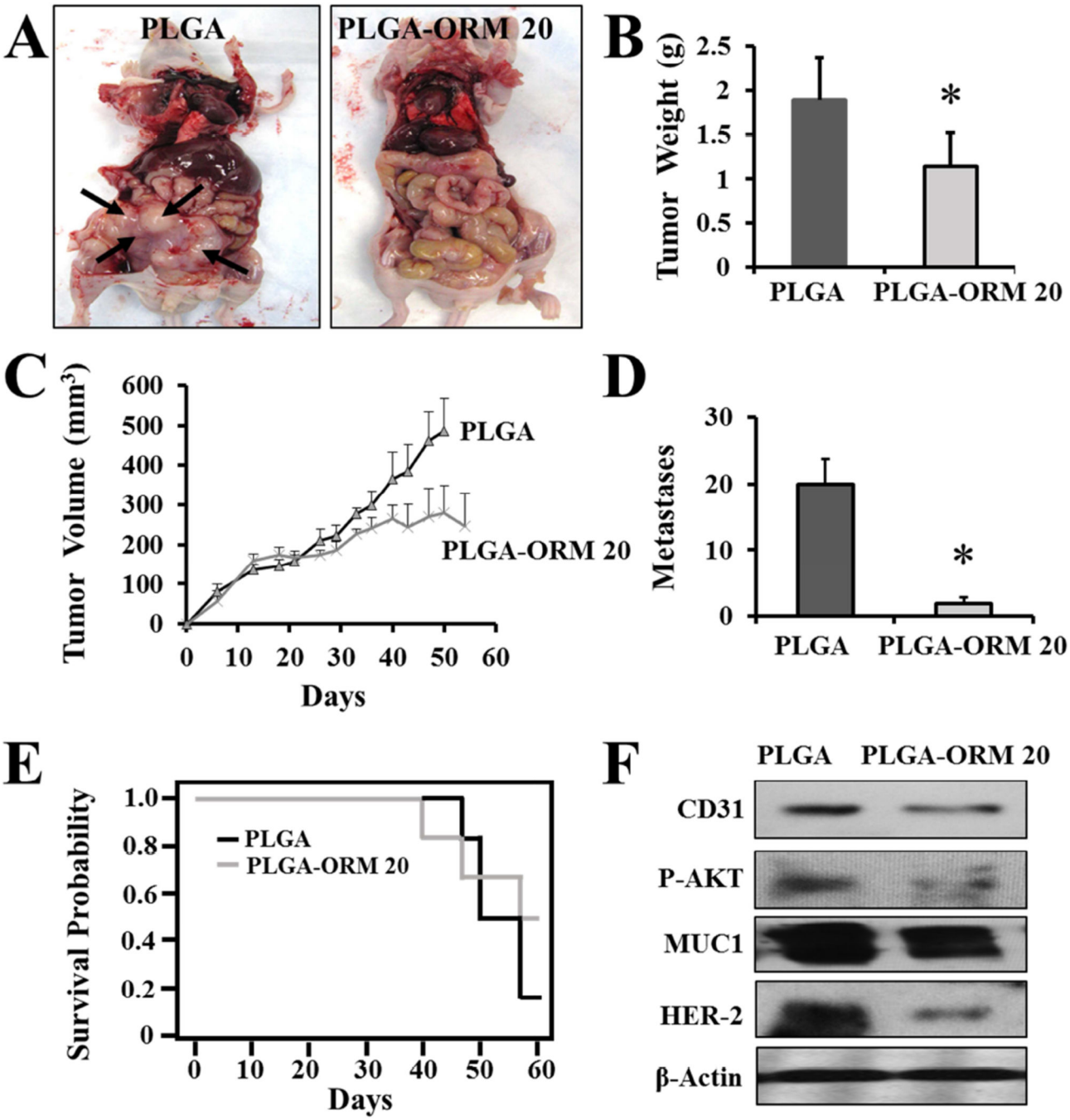

Figure 6. PLGA-ORM NPs inhibit tumor growth and metastases in pancreatic tumor xenograft mice model

Tumor bearing (BxPC-3 human pancreatic xenograft) mice were generated by subcutaneous (5×10^6 cells/animal) and intraperitoneal injection of BxPC-3 cells (3×10^6 cells/animal). The mice were randomly distributed and treated with intraperitoneal injection of PLGA-ORM 20 formulation (equivalent of 200 μg ORM/mouse) or its equivalent PLGA NPs. **(A).** Photographs representing control PLGA and PLGA-ORM 20 treated mice. Note: Control PLGA treated mice showed large tumors with visible metastatic lesions (represented with

black arrows) while PLGA-ORM 20 treated mice did not show any visible metastatic lesions. **(B–C).** Average tumor weight and tumor volume of PLGA and PLGA-ORM 20 treated mice. **(D).** Effect of PLGA-ORM 20 formulation on the number of metastases formed. Bars represent mean ± SD; *$p<0.05$. **(E).** Animal survival curve. Note: Two animals in PLGA-ORM group were died because of bladder puncture not because of cancer or PLGA-ORM NPs treatment. **(F).** Immunoblot analysis of dissected tumors.

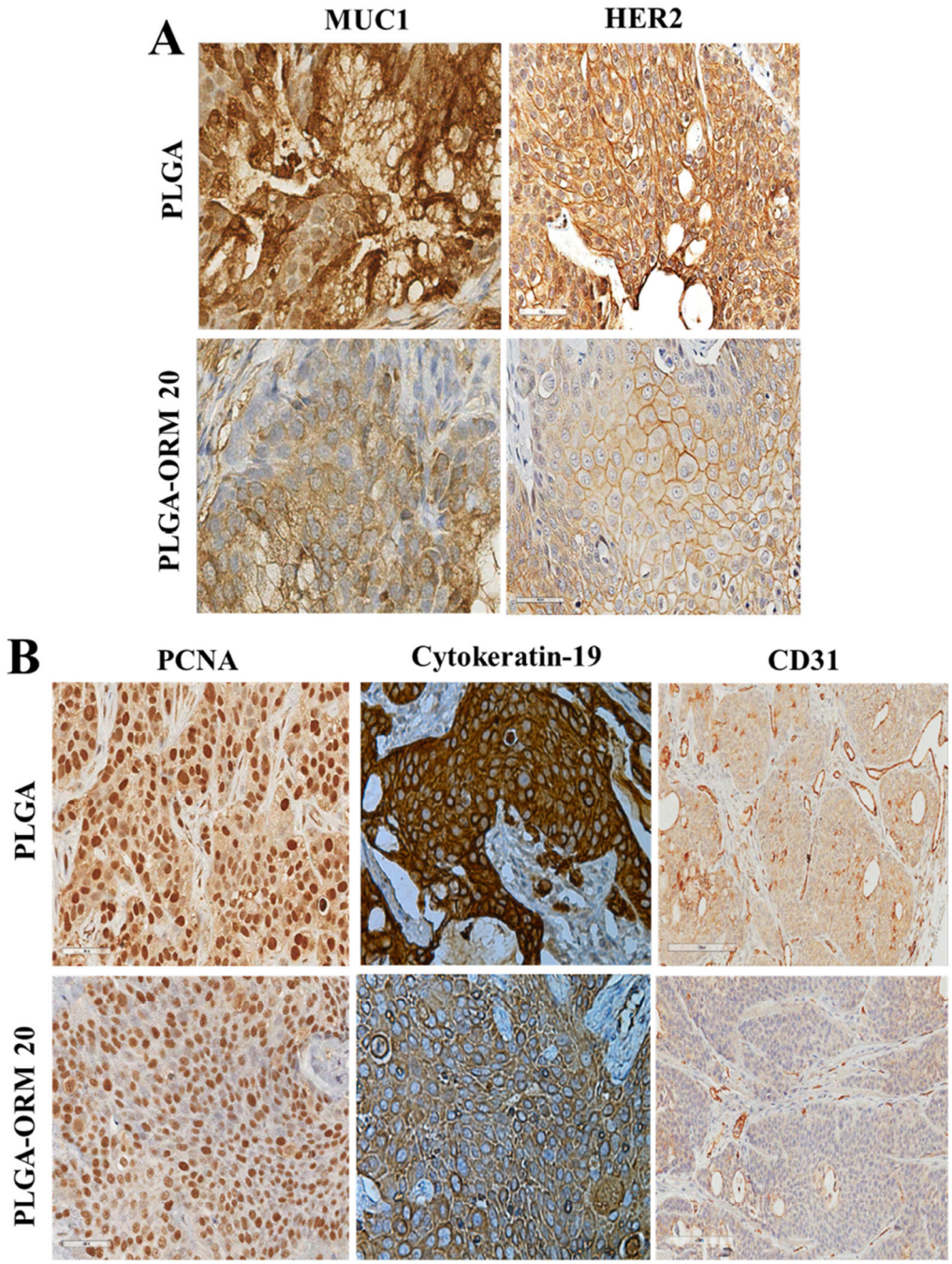

Figure 7. PLGA-ORM NPs significantly inhibit key oncogenic signaling events associated with pancreatic cancer progression

Representative photomicrographs of immunohistochemistry (IHC) analysis of xenograft tumor tissues. Paraffin embedded tumor xenografts were sectioned and immunohistochemically stained for **(A)** MUC1, HER2, and **(B)** PCNA, CK19, and CD31. The results showed reduced staining of tissues for these proteins in PLGA-ORM 20 treated mice as compared to PLGA control group. (Original Magnifications 600×)

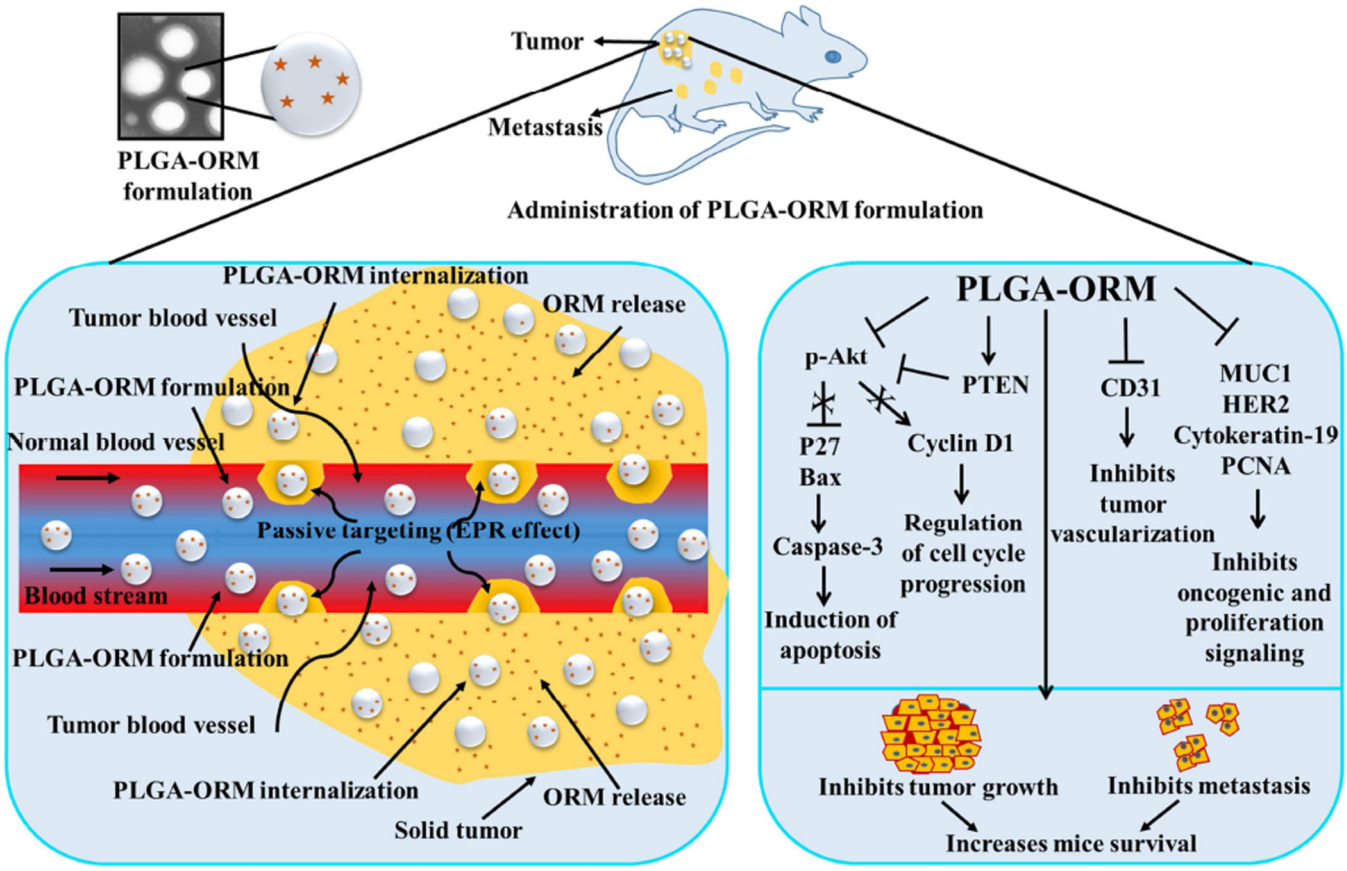

Figure 8.

Schematic representation of EPR effect of PLGA-ORM NPs in pancreatic cancer mouse tumor(s) and possible biological implications. Improved molecular and therapeutic effects of PLGA-ORM NPs achieved in pancreatic cancer mouse model due to significant accumulation of PLGA-ORM NPs and sustained release of ormeloxifene from NPs at the tumor site.

Table 1

Effect of PLGA-ORM 20 formulation on tumor development and dissemination.

Treatment	Effect of PLGA-ORM 20 on tumor development and dissemination					*P-values*
	No. of mice	**% age of mice with secondary tumors**	**Total met counts**	**Mean volume (mm^3) of secondary tumors**	**Mean tumor weight (gm) (pr+sec)**	
PLGA	6	100	80	78.83	1.8	<0.01
PLGA-ORM 20	6	50	11	0	1.1	<0.001
Treatment	**No. of mice with dissemination**					**Av. Metastases**
	Intestine	**Spleen**	**Diaphragm**	**Intraperitoneal cavity**	**Liver**	
PLGA	5	3	4	4	4	20
PLGA-ORM 20	0	2	0	1	0	1.83*

*Significantly different from PLGA group ($p<0.01$)